

Article

A Conservation Voltage Reduction Scheme for a Distribution Systems with Intermittent Distributed Generators

Pyeong-Ik Hwang ¹, Seung-II Moon ² and Seon-Ju Ahn ^{3,*}

¹ Korea Electric Power Research Institute (KEPRI), 105 Munji-Ro, Yuseong-gu, Daejeon 34056, Korea; pyeongik.hwang@kepc.co.kr

² Department of Electrical and Computer Engineering, Seoul National University, 1 Gwanak-ro, Gwank-gu, Seoul 08826, Korea; moonsi@plaza.snu.ac.kr

³ Department of Electrical Engineering, Chonnam National University, 77 Yongbong-ro, Buk-gu, Gwangju 61186, Korea

* Correspondence: sjahn@jnu.ac.kr; Tel.: +82-62-530-1738

Academic Editor: Neville R. Watson

Received: 5 July 2016; Accepted: 17 August 2016; Published: 23 August 2016

Abstract: In this paper, a conservation voltage reduction (CVR) scheme is proposed for a distribution system with intermittent distributed generators (DGs), such as photovoltaics and wind turbines. The CVR is a scheme designed to reduce energy consumption by lowering the voltages supplied to customers. Therefore, an unexpected under-voltage violation can occur due to the variation of active power output from the intermittent DGs. In order to prevent the under-voltage violation and improve the CVR effect, a new reactive power controller which complies with the IEEE Std. 1547TM, and a parameter determination method for the controller are proposed. In addition, an optimal power flow (OPF) problem to determine references for the resources of CVR is formulated with consideration of the intermittent DGs. The proposed method is validated using a modified IEEE 123-node test feeder. With the proposed method, the voltages of the test system are maintained to be greater than the lower bound, even though the active power outputs of the DGs are varied. Moreover, the CVR effect is improved compared to that used with the conventional reactive power control methods.

Keywords: conservation voltage reduction; distributed generator; distribution system; reactive power control; volt/var control

1. Introduction

Driven by advances in information and communications technologies, various next-generation distribution management systems (DMSs) have been proposed for more reliable and efficient operation of a distribution system with distributed generators (DGs), e.g., advanced DMS [1] and smart DMS [2]. In the next-generation DMSs, network-model-based analysis functions, such as topology process and power flow, have been adopted for more reliable and economic operation. The state of the distribution system can be estimated accurately from the measured data and network model including branch parameters. Moreover, operation resources can be controlled remotely via a suitable communication infrastructure.

Volt/var control (VVC), one of the key technologies required for a DMS, maintains the voltages of the distribution system within specified bounds, such as those stated by the American National Standards Institute (ANSI) [3] and Canadian Standards Association (CSA) [4]. Among the various VVC methods, conservation voltage reduction (CVR) is one of the easiest ways to reduce the peak load and total energy consumption and it has become the major function of VVC [5]. The basic idea of CVR is that the active and reactive power demands of a load generally decrease as the supplied voltage

decreases. The decrease in the reactive power demand also reduces the line loss of the distribution system. Consequently, both the active power demand and the line loss can be reduced by lowering the supplied voltages. The first wide-scale CVR was implemented by American Electric Power (AEP) in 1973 [6]. Since then, numerous electric utilities have implemented CVR and its practical effects have been evaluated. It has been reported that energy consumption can be reduced by 0.3%–1.0% by reducing the voltage by 1.0% [5–10].

Traditionally, on-load tap changers (OLTCs) on substation transformers, step voltage regulators (SVRs), and shunt capacitors (ShCs) on distribution feeders are used for CVR. With the recent increase in the interconnection of DGs that can control reactive power, the DGs are also considered as one of the controllable resources for CVR [11–15]. Among various methods to implement CVR, network-model-based methods will likely be adopted for the next-generation DMSs because more reliable and optimal CVR can be achieved. With the network-model-based methods, references for the volt/var control devices are calculated by solving the optimal power flow (OPF), representing CVR in the DMS; these are then sent to each volt/var control device via a communication infrastructure. Since creating a base case for the OPF from measurements and solving the OPF are time consuming, the references are periodically determined with a certain time interval. During the interval, the voltage problems caused by the active power variations of intermittent DGs, such as photovoltaics and wind turbines, should be resolved by local controllers of the DGs, because the conventional devices, such as SVRs and ShCs, are unable to respond to a fast voltage variation [5]. Therefore, in order to implement reliable and optimal CVR for a distribution system with the intermittent DGs, the effect of intermittency should be taken into account in both the OPF of the DMS and the local controller of the DGs.

Recently, uncertainty issues have emerged in distribution system operation [16,17]. In [11–15], while the formulations of the OPF were proposed to utilize the DG for the CVR, the characteristics of the intermittent DGs were not considered. Meanwhile, various reactive power control methods for the intermittent DG have been proposed, e.g., fixed power factor control, variable power factor control [18], fixed voltage control, and advanced reactive power control methods, including volt-var and volt-watt response modes [19]. However, these methods are not optimized for CVR. Therefore, a new CVR method is proposed in this paper for a distribution system with intermittent DGs that includes: (1) OPF formulation for the DMS and (2) reactive power controller for the DGs. With the proposed method, the power references and control parameters for volt/var control devices including the DGs are determined periodically by solving the OPF in the DMS and the reactive power output of the DG is controlled by using the proposed local controller in real-time. The remainder of the paper is divided into five sections and is organized as follows: in Section 2, the requirements for a local reactive power controller of the intermittent DGs to improve the CVR effect are discussed and a new reactive power controller satisfying the requirements is proposed. The OPF formulation method with consideration of the intermittent DGs and a method to determine power references for the proposed controller are presented in Section 3. Section 4 presents a method to determine the control parameters for the proposed controller. In Section 5, the effects of the proposed method are validated from various case studies. Finally, Section 6 contains concluding remarks.

The major contribution of this paper is that a CVR method considering the intermittency of the active power output of the DGs. A reactive power controller of an intermittent DG is designed to maximize CVR effect based on the voltage characteristics of a distribution system. In addition, a method to determine the control parameters for the reactive power controller is proposed not only to maximize the CVR effect but also to prevent an unexpected under voltage violation.

2. Reactive Power Control Method for an Intermittent DG: Local Controller

2.1. Effect of Active Power Variation on Node Voltage

Figure 1a illustrates various examples of node voltage according to the variation of active power output of a DG when the reactive power output is fixed at Q_{DG}^* (reactive power reference determined

by solving the OPF), as shown in Figure 1b. In the OPF of the DMS, Q_{DG}^* is calculated such that the voltages are close to the lower voltage bound (V^{lb}) when the active power output is equal to P_{DG}^* (active power output of the DG for the base case of the OPF). If the active power output is less than P_{DG}^* , voltages will decrease and thus an under-voltage can occur. On the contrary, if the active power output is higher than P_{DG}^* , the effect of CVR will be degraded due to the increase in the voltage. In summary, the reactive power output of the DG should be controlled appropriately according to its active power output for the reliable and efficient CVR.

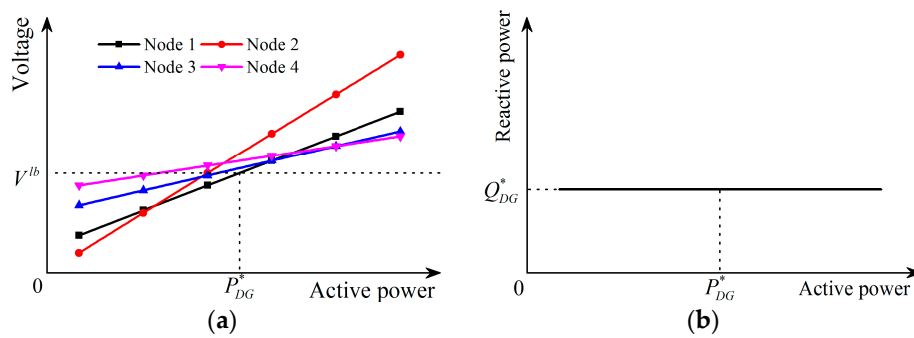


Figure 1. Voltage magnitude and reactive power variation according to active power: Fixed reactive power controller, (a) Voltage magnitude; (b) Reactive power.

2.2. Proposed Reactive Power Controller

Figure 2a shows an ideal voltage profile that maximizes the CVR effect. For this, the reactive power output of a DG should be controlled piecewise linearly according to the active power output as shown in Figure 2b, where, for simplicity of discussion, it is assumed that the voltage magnitude sensitivities of all nodes with respect to the reactive power of the DG are the same in this section. However, since it is difficult to determine the exact active power versus reactive power characteristic for a practical distribution system with many DGs, a simplified version of the aforementioned ideal controller is proposed.

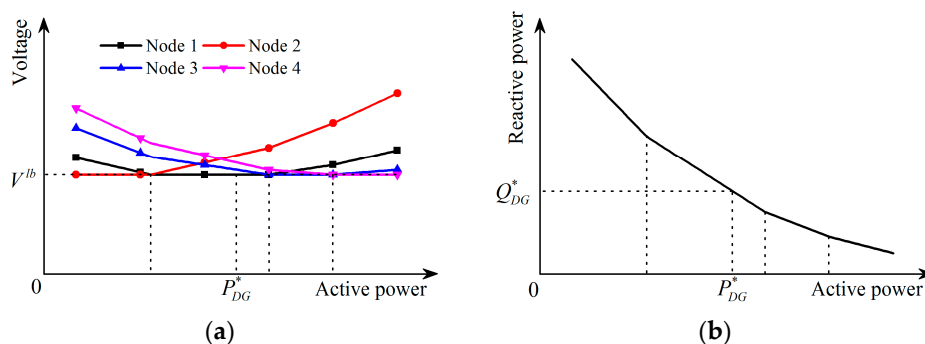


Figure 2. Voltage magnitude and reactive power variation according to active power: Ideal reactive power controller for CVR, (a) Voltage magnitude; (b) Reactive power.

The proposed reactive power controller uses the conventional fixed reactive power controller but the reference (Q_{ref}^{FQ}) is adaptively determined, as shown in Figure 3. In the controller, the reference is calculated from the measured active power output, P_{DG} , as:

$$Q_{ref}^{FQ} = \begin{cases} Q_{ref}^{QP} - R^-(P_{DG} - P_{ref}^{QP}) & \text{If } P_{DG} < P_{ref}^{QP} \\ Q_{ref}^{QP} - R^+(P_{DG} - P_{ref}^{QP}) & \text{Otherwise} \end{cases} \quad (1)$$

where Q_{ref}^{QP} and P_{ref}^{QP} are the reactive and active power references, respectively, and R^- and R^+ are the lower and upper droop constants, respectively. If the active power output is smaller than the reference value, the lower droop constant will be used to determine the reactive power output; otherwise, the upper droop constant is used. The proposed controller complies with the IEEE Std. 1547TM [20] (which specifies the standard for interconnecting DGs), because it does not actively regulate the voltage of the point of common coupling (PCC). Since the power references and the droop constants should be determined with consideration of the state of the distribution system, these should be calculated in the next-generation DMS as shown in Figure 3. The calculation method will be presented in the next section.

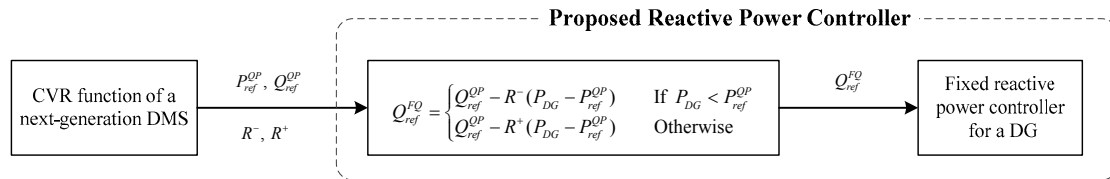


Figure 3. Outline of the proposed reactive power controller.

If the active power output of the DG is equal to P_{DG}^* , the reactive power output should be identical to Q_{DG}^* . Therefore, Q_{ref}^{QP} and P_{ref}^{QP} are set at Q_{DG}^* and P_{DG}^* , respectively. The relationship between the active and reactive power outputs of the proposed controller is illustrated in Figure 4b, and with proper droop constants, the voltages can be controlled as shown in Figure 4a. Since the reactive power output is determined by two line segments given by the droop constants and the references, the proposed controller will be referred to as the “two-segment reactive power versus active power (Q–P) droop controller”.

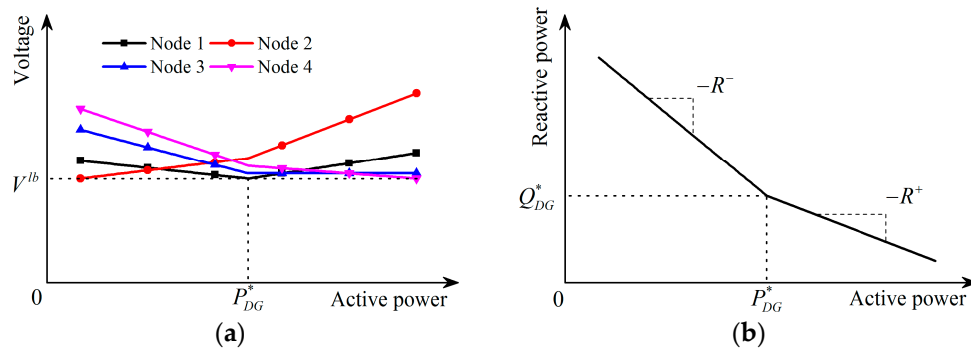


Figure 4. Voltage magnitude and reactive power variation according to active power: Proposed reactive power controller, (a) Voltage magnitude; (b) Reactive power.

3. Power Reference Determination: DMS Function

Since the aim of CVR is to reduce the energy consumption of a distribution system, the problem can be formulated as follows [21].

$$\text{Minimize } P_s \tag{2}$$

subject to:

$$P_i = V_i \sum_k V_k (G_{ik} \cos(\theta_i - \theta_k) + B_{ik} \sin(\theta_i - \theta_k)) \tag{3}$$

$$Q_i = V_i \sum_k V_k (G_{ik} \sin(\theta_i - \theta_k) - B_{ik} \cos(\theta_i - \theta_k)) \tag{4}$$

$$x_i^{lb} \leq x_i \leq x_i^{ub} \tag{5}$$

where P_s is the active power drawn from the substation, P_i and Q_i are the active and reactive powers injected by loads and DGs connected to node i , V_i and θ_i are the voltage magnitude and angle of node i , G_{ik} and B_{ik} are the real and imaginary parts of the bus admittance matrix, x is the decision variable, and x_i^{lb} and x_i^{ub} are the lower and upper bounds of the decision variable i . The decision variables consist of references for the volt/var control devices, such as tap positions for the SVRs and OLTCs, states of ShCs, reactive power outputs of DGs, and the voltage magnitudes and angles. Because the reduction of the active power consumption is identical to the reduction of the energy consumption in point of CVR, the objective function is formulated in terms of active power. Because the optimization problem includes power flow Equations (3) and (4), it is classified as an OPF problem [22]. In the CVR problem, the DGs connected to low voltage network, less than 1 kV, are not considered because general DMSs do not control them directly. However, if a DMS should control all DGs including the DGs connected to the low voltage network, the proposed method can be used by adopting aggregated DG models for the DGs connected to the low voltage network.

Due to the large number of possible combinations of active power outputs of the intermittent DGs, it is almost impossible to determine both the references for the volt/var control devices and the droop constants for the proposed controller to ensure no voltage problem by solving a single OPF. Therefore, in the proposed method, the problems are decoupled. The references are first determined by solving the OPF given by Equations (2)–(5). Then, the droop constants are calculated from the optimal solution of the OPF by using the method presented in the next sections. In this section, the modifications of the OPF formulation to consider intermittent DGs and the power reference determination from the optimal solution of the OPF are presented.

3.1. Modifications of the OPF

Since the references are determined by solving the OPF, the base case of the OPF should be carefully chosen. If the measured active power output of the intermittent DG that can vary rapidly and randomly is directly used to generate the base case, the reference value of the mechanical switch based volt/var control devices can change frequently. The frequent switching operation of devices such as OLTCs and SVCs will reduce their lifetime and the system operation cost will thus be increased. Therefore, an appropriate value that changes slowly and gradually over time should be used as the active power output of the DG for the base case.

The change in the expected value of the active power output with respect to time is slow and gradual. Thus, the expected value is used for the base case in the proposed method:

$$P_{DG,k}^* = E[P_{DG,k}] \quad (6)$$

where $P_{DG,k}^*$ is the active power output of DG k for the base case, $P_{DG,k}$ is the active power output of DG k , and $E[\cdot]$ is the expected value operator. The expected value can be obtained from a forecasted probability density function (PDF) or historical data [23].

For a dispatchable DG, the reactive power reference should be in the range determined by specific power factors, as given by a grid code [24]. Therefore, the reactive power limits for the intermittent DG are also determined based on the power factors:

$$Q_{DG,k}^{min} = -P_{DG,k}^* \tan \left(\cos^{-1} (pf_{lead}) \right) \quad (7)$$

$$Q_{DG,k}^{max} = P_{DG,k}^* \tan \left(\cos^{-1} (pf_{lag}) \right) \quad (8)$$

where $Q_{DG,k}^{min}$ and $Q_{DG,k}^{max}$ are the minimum and maximum limits of the reactive power of DG k for the OPF and pf_{lead} and pf_{lag} are the minimum leading power factor and the minimum lagging power factor, respectively. Consequently, if the active power output of the intermittent DG is not varied, it is treated as the same as a dispatchable DG.

3.2. Power Reference Determination

It is clear that the reactive power of the DG should be identical to that of the optimal solution of the OPF, $Q_{DG,k}^*$, if the active power is identical to that of the base case of the OPF, $P_{DG,k}^*$. Therefore, the active and reactive power references for the proposed reactive power controller of DG k are set at $P_{DG,k}^*$ and $Q_{DG,k}^*$, respectively, i.e., $P_{ref,k}^{QP} = P_{DG,k}^*$ and $Q_{ref,k}^{QP} = Q_{DG,k}^*$.

4. Droop Constant Determination: DMS Function

If the lower droop constant is too small or the upper droop constant is too large, the DG cannot supply enough reactive power to keep the voltages above the lower voltage bound. In the opposite case, the voltages will be excessively increased due to the excessive reactive power supply and thus the effect of CVR will be degraded. Therefore, to achieve the best effect of CVR while ensuring no under-voltage violation, a two-stage method to determine the optimal droop constant is proposed: (1) initial estimation and (2) final correction. In the initial estimation stage, the droop constants are determined considering only the active power output variation of a single DG. Then, in the final correction stage, the droop constants are refined considering the active power variation of multiple DGs.

4.1. Initial Estimation

Voltage variations due to an active power change of a DG should be compensated for by the DG itself since voltage measurements are not used in the proposed controller. When the active and reactive power outputs of only one DG k , $P_{DG,k}$ and $Q_{DG,k}$, change while those of the other DGs are fixed at the values given by the OPF, the voltage magnitude of node i can be approximated as:

$$V_i \approx V_i^* + \left. \frac{\partial V_i}{\partial P_{DG,k}} \right|_* (P_{DG,k} - P_{DG,k}^*) + \left. \frac{\partial V_i}{\partial Q_{DG,k}} \right|_* (Q_{DG,k} - Q_{DG,k}^*) \quad (9)$$

where $\left. \frac{\partial V_i}{\partial P_{DG,k}} \right|_*$ and $\left. \frac{\partial V_i}{\partial Q_{DG,k}} \right|_*$ are the voltage magnitude sensitivities of node i with respect to the active and reactive power outputs of DG k , respectively, at the optimal operating point determined by the OPF. The sensitivities can be calculated by using Jacobian matrix.

In the proposed controller, $P_{DG,k}^*$ and $Q_{DG,k}^*$ are used as the active and reactive power references, and it can be assumed that the reactive power output is the same as the reference value in the steady-state. If the active power output is less than the reference value, i.e., $P_{DG,k} < P_{DG,k}^*$, the lower droop constant will be used and the voltage magnitude of node i can be written as follows:

$$V_i \approx V_i^* + \left. \frac{\partial V_i}{\partial P_{DG,k}} \right|_* (P_{DG,k} - P_{DG,k}^*) - R_k^- \left. \frac{\partial V_i}{\partial Q_{DG,k}} \right|_* (P_{DG,k} - P_{DG,k}^*) \quad (10)$$

Therefore, the minimum voltage constraint for node i can be written as:

$$V_i^{lb} \leq V_i^* + \left. \frac{\partial V_i}{\partial P_{DG,k}} \right|_* (P_{DG,k} - P_{DG,k}^*) - R_k^- \left. \frac{\partial V_i}{\partial Q_{DG,k}} \right|_* (P_{DG,k} - P_{DG,k}^*) \quad (11)$$

Since power systems are designed and operated so that the voltage magnitude sensitivity with respect to the reactive power is always positive [25], the constraint for the lower droop constant can be formulated as follows by rearranging Equation (11):

$$R_k^- \geq \frac{V_i^* - V_i^{lb}}{\left. \frac{\partial V_i}{\partial Q_{DG,k}} \right|_* (P_{DG,k} - P_{DG,k}^*)} + \left. \frac{\partial V_i}{\partial P_{DG,k}} \right|_* \quad (12)$$

Because V_i^* is always greater than or equal to V_i^{lb} , the value of the right-hand side of the inequality will be the maximum when the active power output is equal to the minimum value, $P_{DG,k}^{min}$. Therefore, the constraint is modified as:

$$R_k^- \geq \frac{V_i^* - V_i^{lb}}{\frac{\partial V_i}{\partial Q_{DG,k}} \Big|_* (P_{DG,k}^{min} - P_{DG,k}^*)} + \frac{\frac{\partial V_i}{\partial P_{DG,k}} \Big|_*}{\frac{\partial V_i}{\partial Q_{DG,k}} \Big|_*} \quad (13)$$

The initial lower droop constant for DG k is determined as follows because the minimum voltage constraint should be satisfied for all nodes.

$$R_k^- = \max_i \left\{ \frac{V_i^* - V_i^{lb}}{\frac{\partial V_i}{\partial Q_{DG,k}} \Big|_* (P_{DG,k}^{min} - P_{DG,k}^*)} + \frac{\frac{\partial V_i}{\partial P_{DG,k}} \Big|_*}{\frac{\partial V_i}{\partial Q_{DG,k}} \Big|_*} \right\} \quad (14)$$

From the similar procedure, the initial upper droop constant can be given by:

$$R_k^+ = \min_i \left\{ \frac{V_i^* - V_i^{lb}}{\frac{\partial V_i}{\partial Q_{DG,k}} \Big|_* (P_{DG,k}^{max} - P_{DG,k}^*)} + \frac{\frac{\partial V_i}{\partial P_{DG,k}} \Big|_*}{\frac{\partial V_i}{\partial Q_{DG,k}} \Big|_*} \right\} \quad (15)$$

where $P_{DG,k}^{min}$ is the possible maximum active power output of DG k . The overall procedure to determine the initial droop constants is summarized in Figure 5.

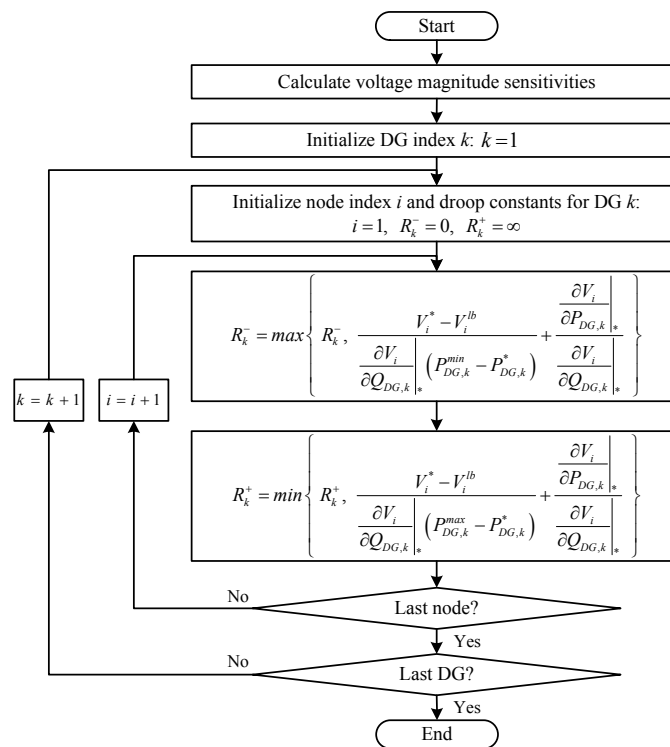


Figure 5. Flow chart of the initial estimation.

4.2. Final Correction

Since the droop constants are calculated considering the active power variation of a single DG in the initial estimation, an under-voltage violation can occur when active power outputs of two or more DGs vary simultaneously. Therefore, the droop constants should be corrected with the consideration of the active power output changes of multiple DGs.

Figure 6 shows examples of the possible node voltage trajectory according to the active power output change of the DG when the two-segment Q–P droop controller is adopted.

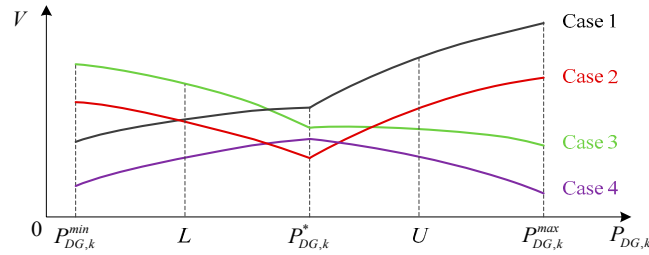


Figure 6. Possible trajectory of the node voltage magnitude with the two-segment Q–P droop controller.

As shown in the figure, the gradient can be changed drastically at the reference active power. Therefore, two sets of the sensitivities calculated at two representative operating points, denoted as “L” and “U”, are used to correct the droop constants in the proposed method. At “L”, active power outputs of DGs are given by:

$$P_{DG,k}^L = \frac{P_{DG,k}^{min} + P_{DG,k}^*}{2} \quad \text{for all DG } k \quad (16)$$

Since the active power output is smaller than its reference value, the reactive power output is determined as:

$$Q_{DG,k}^L = Q_{DG,k}^* - R_k^- \left(P_{DG,k}^L - P_{DG,k}^* \right) \quad \text{for all DG } k \quad (17)$$

At the operating point “U”, the active and reactive power outputs are given by:

$$P_{DG,k}^U = \frac{P_{DG,k}^{max} + P_{DG,k}^*}{2} \quad \text{for all DG } k \quad (18)$$

$$Q_{DG,k}^U = Q_{DG,k}^* - R_k^+ \left(P_{DG,k}^U - P_{DG,k}^* \right) \quad \text{for all DG } k \quad (19)$$

By using the sensitivities calculated at the operating points and (10), the gradients of the voltage magnitude of node *i* with respect to the active power output of DG *k* can be approximated as:

$$G_{ik}^- = \left. \frac{\partial V_i}{\partial P_{DG,k}} \right|_L - R_k^- \left. \frac{\partial V_i}{\partial Q_{DG,k}} \right|_L$$

$$G_{ik}^+ = \left. \frac{\partial V_i}{\partial P_{DG,k}} \right|_U - R_k^+ \left. \frac{\partial V_i}{\partial Q_{DG,k}} \right|_U \quad (21)$$

where G_{ik} is the gradient when the active power output is smaller than its reference, G_{ik}^+ is the gradient when the active power output is larger than its reference, and $(\cdot)|_L$ and $(\cdot)|_U$ refer to the sensitivities calculated at operating points “L” and “U”, respectively.

From the gradients, the active power output that minimizes the voltage magnitude can be inferred. For example, if both of the gradients are positive (i.e., Case 1 shown in Figure 6), the minimum voltage occurs when the active power output is equal to its minimum. For all possible cases, the active power output of DG *k*, $P_{DG,k} = P_{DG,k}^* + P_{DG,k}^- + P_{DG,k}^+$, can be determined:

$$G_{ik}^- \geq 0 \ \& \ G_{ik}^+ \geq 0 \text{ (Case 1): } \Delta P_{DG,k}^- = P_{DG,k}^{min} - P_{DG,k}^*, \ \Delta P_{DG,k}^+ = 0$$

$$G_{ik}^- < 0 \ \& \ G_{ik}^+ \geq 0 \text{ (Case 2): } \Delta P_{DG,k}^- = 0, \ \Delta P_{DG,k}^+ = 0$$

$$G_{ik}^- < 0 \ \& \ G_{ik}^+ < 0 \text{ (Case 3): } \Delta P_{DG,k}^- = 0, \ \Delta P_{DG,k}^+ = P_{DG,k}^{max} - P_{DG,k}^*$$

$$G_{ik}^- \geq 0 \ \& \ G_{ik}^+ < 0 \text{ (Case 4):}$$

$$\text{If } G_{ik}^- (P_{DG,k}^{min} - P_{DG,k}^*) \leq G_{ik}^+ (P_{DG,k}^{max} - P_{DG,k}^*): \Delta P_{DG,k}^- = P_{DG,k}^{min} - P_{DG,k}^*, \ \Delta P_{DG,k}^+ = 0$$

Otherwise: $\Delta P_{DG,k}^- = 0$, $\Delta P_{DG,k}^+ = P_{DG,k}^{max} - P_{DG,k}^*$.

Using the gradients and the active power outputs, the minimum voltage magnitude can be estimated as:

$$\tilde{V}_i^{min} \approx V_i^* + \sum_k \left[G_{ik}^- \Delta P_{DG,k}^- + G_{ik}^+ \Delta P_{DG,k}^+ \right] \quad (22)$$

If the estimated minimum voltage is less than the lower bound, the droop constants should be modified to eliminate the under-voltage violation. If the lower droop constant is activated (i.e., $P_{DG,k}^- < 0$), the lower droop constant should be increased. On the contrary, if the upper constant is activated (i.e., $P_{DG,k}^+ > 0$), the upper droop constant should be reduced. In the proposed method, only the activated droop constants are corrected as:

$$R_k^- = \begin{cases} (1 + \alpha) R_k^- & \text{if } \Delta P_{DG,k}^- < 0 \\ R_k^- & \text{Otherwise} \end{cases} \quad (23)$$

$$R_k^+ = \begin{cases} (1 - \alpha) R_k^+ & \text{if } \Delta P_{DG,k}^+ > 0 \\ R_k^+ & \text{Otherwise} \end{cases} \quad (24)$$

where α is a positive constant.

The voltage magnitude with the corrected droop constants can be approximated as follows because $P_{DG,k}^-$ and $P_{DG,k}^+$ corresponding to inactivated droop constants are zero:

$$\tilde{V}_i^{corr} \approx V_i^* + \sum_k \left[\left(\left. \frac{\partial V_i}{\partial P_{DG,k}} \right|_L - (1 + \alpha) R_k^- \left. \frac{\partial V_i}{\partial Q_{DG,k}} \right|_L \right) \Delta P_{DG,k}^- + \left(\left. \frac{\partial V_i}{\partial P_{DG,k}} \right|_U - (1 - \alpha) R_k^+ \left. \frac{\partial V_i}{\partial Q_{DG,k}} \right|_U \right) \Delta P_{DG,k}^+ \right] \quad (25)$$

From Equations (20)–(22), the corrected voltage can be written as:

$$\tilde{V}_i^{corr} \approx \tilde{V}_i^{min} - \alpha \sum_k \left(R_k^- \left. \frac{\partial V_i}{\partial Q_{DG,k}} \right|_L \Delta P_{DG,k}^- - R_k^+ \left. \frac{\partial V_i}{\partial Q_{DG,k}} \right|_U \Delta P_{DG,k}^+ \right) \quad (26)$$

Because the corrected voltage should be equal to the lower bound ($\tilde{V}_i^{corr} = V_i^{lb}$) to maximize the CVR effect, α is given by:

$$\alpha = \frac{V_i^{lb} - \tilde{V}_i^{min}}{-\sum_k \left(R_k^- \left. \frac{\partial V_i}{\partial Q_{DG,k}} \right|_L \Delta P_{DG,k}^- - R_k^+ \left. \frac{\partial V_i}{\partial Q_{DG,k}} \right|_U \Delta P_{DG,k}^+ \right)} \quad (27)$$

Finally, the droop constants are corrected by using Equations (23) and (24). Even though the corrected droop constants are used, the voltage magnitude of node i can be smaller than its lower bound for another combination of the active power outputs. Therefore, the procedure is repeated until the estimated minimum voltage magnitude given by Equation (22) is larger than or equal to the lower bound. The overall procedure used to correct the droop constants is summarized in Figure 7.

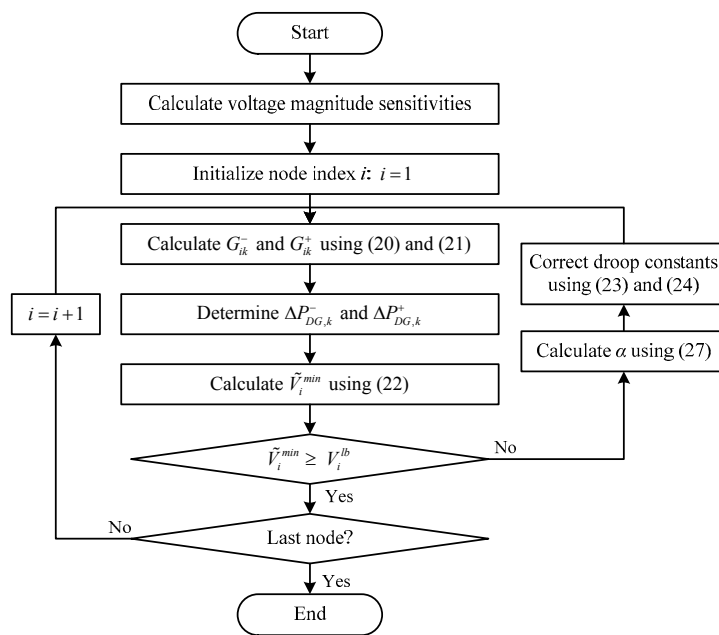


Figure 7. Flow chart of the final correction.

5. Case Studies

Two test systems based on the IEEE 123-node test feeder shown in Figure 8 were used to validate the effects of the proposed method [26]:

Two-DG system: two three-phase 1.5-MW DGs are connected to nodes 66 (DG1) and 250 (DG2) of the original system via transformers (1.7 MVA, 4.16/0.69 kV, 0+j1%).

Five-DG system: five three-phase 1.0-MW DGs are connected to nodes 49, 66, 89, 250, and 300 via transformers (1.2 MVA, 4.16/0.69 kV, 0+j1%).

It was assumed that the two voltage regulators (VRs) circled in Figure 8, VR 1 and VR 4, together with all DGs, were utilized to implement the CVR. With the two-DG system, the effects of the proposed method were investigated in detail by comparing the effects with those of the conventional reactive power control methods, i.e., fixed reactive power (FQ) control and fixed voltage (FV) control. The aim of the test with the five-DG system is to show that the proposed method is also effective for a distribution system with many DGs.

Because the OPF given by Equations (2)–(5) is a mixed integer problem, it was solved by using the predictor and corrector interior point method [27] and the branch and bound method [28]. The operational lower and upper bounds of voltages for all nodes were 0.95 p.u. and 1.05 p.u., respectively. During the OPF procedure, the minimum leading and lagging power factors of the DGs were set at 0.9. In order to calculate the steady-state voltage variation of nodes, the forward/backward sweep power flow method was used [29]. In the power flow, the DGs were represented by using the type 1 model presented in [30]. For the reactive power adjustment of the voltage-controlled DG in the power flow, the method proposed in [31] was adopted.

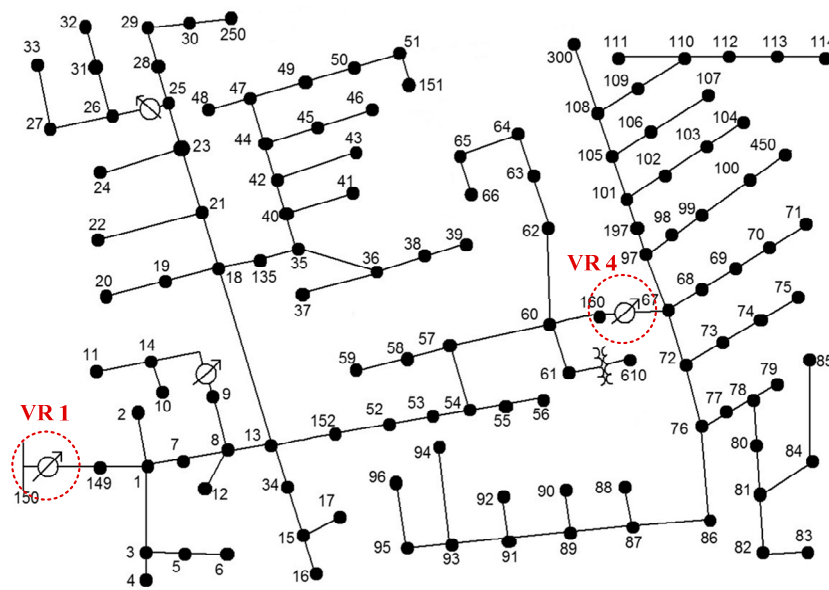


Figure 8. IEEE 123-node test feeder.

5.1. Voltage Control Capability: Two-DG System

The load models (ZIP model) and power consumption of each load were set as identical to those of the original IEEE 123-node system and the expected active power outputs of the DGs were 750 kW, which is 50% of the rated value. By solving the OPF, the tap position references for VRs and the references for DGs were determined as shown in Tables 1 and 2, respectively. Since the FV controller is designed to maintain the measured positive-sequence voltage at the reference value [31], the reference was set to be the same as the positive-sequence voltage calculated from the OPF. The droop constants for the proposed two-segment $Q-P$ droop controller are summarized in Table 3. In the final correction, the droop constants were changed by up to 21.7% from the initial values.

Table 1. References for Reactive Power Controllers.

VRs	Phase A	Phase B	Phase C
VR1	1	-5	-2
VR4	3	1	1

Table 2. References for Reactive Power Controllers.

Controller	DG 1	DG 2
FQ	$Q_{ref}^{FQ} = 171.7 \text{ kVAr}$	$Q_{ref}^{FQ} = 110.6 \text{ kVAr}$
FV	$V_{ref} = 0.9635 \text{ p.u.}$	$V_{ref} = 0.9636 \text{ p.u.}$
Proposed $Q-P$ droop	$P_{ref}^{QP} = 750 \text{ kW}; Q_{ref}^{QP} = 171.7 \text{ kVAr}$	$P_{ref}^{QP} = 750 \text{ kW}; Q_{ref}^{QP} = 110.6 \text{ kVAr}$

Table 3. Droop Constants for DGs (Unit: VAr/W).

DG	Initial Value		Final Value	
	R^-	R^+	R^-	R^+
DG 1	0.3885	0.2424	0.4276	0.2013
DG 2	0.3533	0.2002	0.3997	0.1567

In order to analyze the effect of the intermittent active power output of the DGs on the voltage variation, the minimum voltage of the test system was observed by changing the active power output of each DG by 75 kW. The contour plots of the minimum voltage according to the control methods are shown in Figure 9. The regions filled with blue colors denote that the voltage is less than its lower bound.

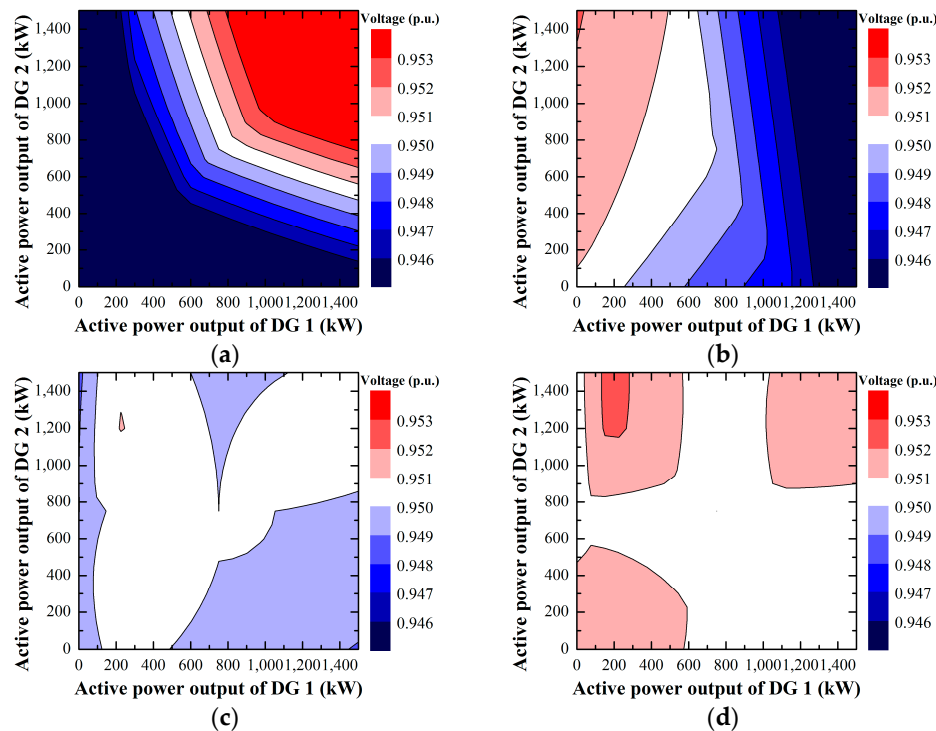


Figure 9. Contours of the minimum voltage (QP : two-segment Q – P droop control), (a) fixed reactive power; (b) fixed voltage; (c) QP w/initial droop constant; (d) QP w/final droop constant.

With the conventional FQ and FV control methods, under-voltage violations occurred in more than half of the cases. Moreover, even though the active power outputs were increased, under-voltage violations occurred with the FV control method as shown in Figure 9b. This is because the voltage controller only maintains the positive-sequence voltage rather than each phase voltage under unbalanced operating conditions. In other words, phase voltages were varied according to the active power output, even though the positive-sequence voltage was maintained at its reference value. In the worst case, the minimum voltage was decreased to 0.9331 p.u. with the FQ control method and to 0.9420 p.u. with the FV control method. The magnitudes of the under-voltage violation (1.69% with FQ control and 0.80% with FV control) are larger than the tap size of a general step voltage regulator, 0.625%.

When the initial droop constants were used for the proposed two-segment Q – P droop controller, the minimum voltage was increased but under-voltage violations still occurred in some cases as shown in Figure 9c and the minimum voltage was decreased to 0.9487 p.u. in the worst case. However, the minimum voltage was always greater than or equal to the lower bound when the proposed controller with the final droop constants determined by using the proposed method was used, as shown in Figure 9d.

5.2. CVR Effect: Two-DG System

In order to assess the CVR effect, the CVR results with the proposed method were compared to those with the conventional reactive power control methods. The DGs were assumed to be photovoltaic. According to the PDF of the active power output for the DG, the three cases shown in Figure 10 were

considered. The PDFs were generated based on the beta distribution function [32]. The minimum and maximum active power outputs for all cases are 0 kW and 1500 kW, respectively. The expected active power outputs of Cases 1, 2, and 3 are 600.0 kW, 857.1 kW, and 1090.9 kW, respectively. Case 1 corresponds to a very cloudy day, while Case 3 corresponds to a slightly cloudy day.

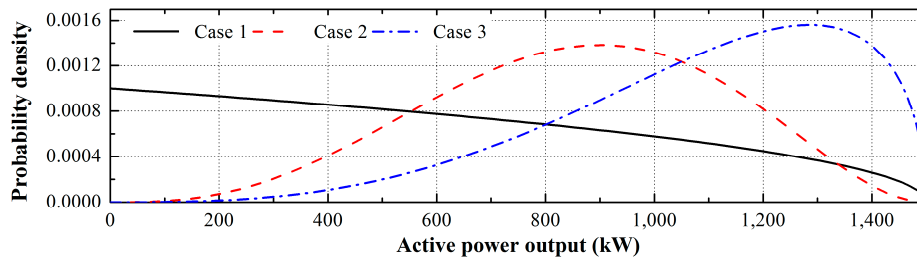


Figure 10. PDFs for the active power output of the DG.

The loads were identical to those of the original system and the active power outputs of the DGs were set at their expected values. The initial states of the volt/var control devices were determined by solving the OPF with the lower voltage bound of 1.0 p.u. Initially, the active power drawn from the substation for Cases 1, 2, and 3 was 2363.0 kW, 1840.8 kW, and 1372.4 kW, respectively. For CVR, the lower voltage bound was set at 0.95 p.u. Therefore, the following results correspond to the CVR effect by reducing the lower bound of voltages by 0.05 p.u. (5%).

As shown in the previous section, an under-voltage violation can occur with the conventional methods. Because the top prior objective of CVR as a VVC method is to maintain the voltages of all nodes within their operational bounds, the references with these methods were determined using the following steps:

- (1) Set the lower voltage bound used for the OPF at the real value (i.e., 0.95 p.u.).
- (2) Solve the OPF and determine the references for DGs.
- (3) Check whether or not an under-voltage violation occurs based on four combinations of the active power outputs: $(P_{DG,1}^{min}, P_{DG,2}^{min})$, $(P_{DG,1}^{min}, P_{DG,2}^{max})$, $(P_{DG,1}^{max}, P_{DG,2}^{min})$, and $(P_{DG,1}^{max}, P_{DG,2}^{max})$.
- (4) If an under-voltage violation is detected, increase the lower bound by 0.0001 p.u. and go to step 2. Otherwise, terminate the procedure.

Since an under-voltage violation can occur not only when the active power output of a DG is minimum but also when the active power output is maximum, all possible combinations of the minimum and maximum active power outputs were tested in step 3. References for VRs and DGs were determined as shown in Tables 4 and 5, respectively. In order to demonstrate the intermittency of the active power output, 100,000 sets of active power outputs were generated based on the PDFs. For each, the minimum voltage and the active power drawn from the substation, which is the objective function to be minimized for CVR, were obtained.

Table 4. Tap References for VRs.

Device	Phase	Case 1			Case 2			Case 3		
		FQ	FV	QP	FQ	FV	QP	FQ	FV	QP
VR 1	A	4	3	1	3	1	0	2	0	-1
	B	-2	-3	-5	-3	-5	-6	-4	-6	-7
	C	1	0	-2	0	-2	-3	-1	-3	-4
VR 4	A	3	3	3	3	3	3	3	3	3
	B	1	1	1	1	1	1	1	1	1
	C	1	1	1	1	1	1	1	2	1

FQ: fixed reactive power control, FV: fixed voltage control, QP: two-segment Q-P droop control.

Table 5. References for DGs.

Device	Method	Reference	Case 1	Case 2	Case 3
DG 1	FQ	Q_{ref}^{FQ} (kVAr)	126.7	186.4	305.7
	FV	V_{ref} (p.u.)	0.9695	0.9728	0.9709
	QP	P_{ref}^{QP} (kW)	600.0	857.1	1090.9
		Q_{ref}^{QP} (kVAr)	197.2	236.8	276.7
		R^- (VAr/W)	0.4577	0.3898	0.3629
		R^+ (VAr/W)	0.2293	0.2448	0.1687
DG 2	FQ	Q_{ref}^{FQ} (kVAr)	87.8	281.7	358.6
	FV	V_{ref} (p.u.)	0.9722	0.9741	0.9734
	QP	P_{ref}^{QP} (kW)	600.0	857.1	1090.9
		Q_{ref}^{QP} (kVAr)	187.1	249.9	354.1
		R^- (VAr/W)	0.3958	0.3753	0.3473
		R^+ (VAr/W)	0.1751	0.1609	0.1553

FQ: Fixed Reactive Power Control, FV: Fixed Voltage Control, QP: Two-Segment Q-P Droop Control.

For all cases, the minimum voltage was larger than or equal to its lower bound. For example, the contour of the minimum voltage for Case 2 is shown in Figure 11, where “E” denotes the minimum voltage when the active power outputs of the DGs are equal to their expected values.

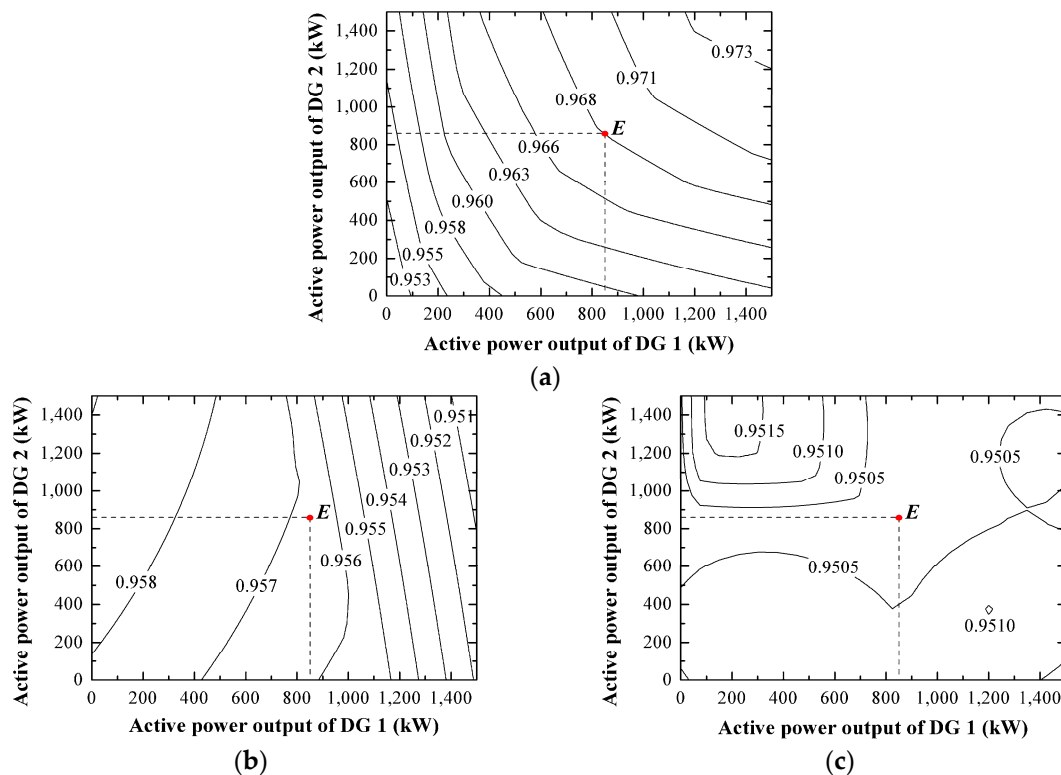


Figure 11. Contour of the minimum voltage for Case 2: Two-DG system, (a) fixed reactive power control; (b) fixed voltage control; (c) Proposed control.

It was observed that the values of “E” for the FQ and FV control methods were larger than the lower bound, while it was equal to the lower bound with the proposed method. In other words, the CVR effect when DGs generate the expected output can be optimized with the proposed method

while ensuring no under-voltage violation. As a result, the active power drawn from the substation was reduced further by using the proposed method as shown in Figure 12. In summary, the CVR effect (i.e., reduction of the active power) was improved by 40.1%–62.6% and 6.8%–23.8% compared with those of the FQ and FV control method, respectively.

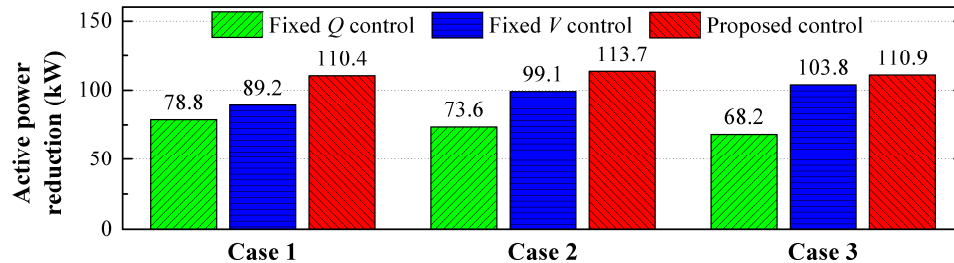


Figure 12. Average reduction of the active power drawn from substation: two-DG system.

5.3. Five-DG System

Three cases were tested according to the load level. The power consumption of each load for Cases 1, 2, and 3 was 70%, 100%, and 130% of the original value, respectively. For the output pattern of DGs, the same PDF as that of Case 3 of the two-DG system with the maximum power of 1000 kW was used. The expected active power output was 727.3 kW. In this case study, the results with the proposed method were only compared to those with the FV method.

In order to identify the voltage control capability, the minimum voltage was obtained by increasing the active power output of each DG by 100 kW. Even though the number of DGs increased, the voltages of the test system were maintained as greater than or equal to the lower bound in all three cases. Only the simulation results for Case 2 are shown in Figure 13 due to limited space. With the FV method, the minimum voltage at the expected operating point was 0.9566 p.u. and the minimum voltage was equal to the lower bound when the active power output of the DG connected to node 66 was maximum and the active power outputs of the other DGs were minimum (i.e., the total active power output was 1000 kW). However, with the proposed method, the minimum voltage was identical to the lower bound at the expected operating point.

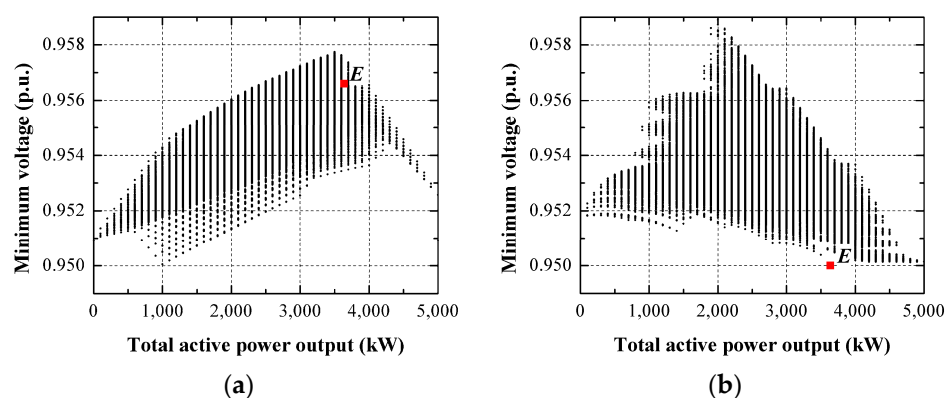


Figure 13. Minimum voltage according to the total active power output of DGs: Case 2 for Five-DG system, (a) FV control; (b) proposed control.

Based on the PDF, one million combinations of active power outputs were generated and tested to validate the effect of CVR. With the proposed method, the active power drawn from the substation was further reduced compared to that with the FV method, as shown in Figure 14.

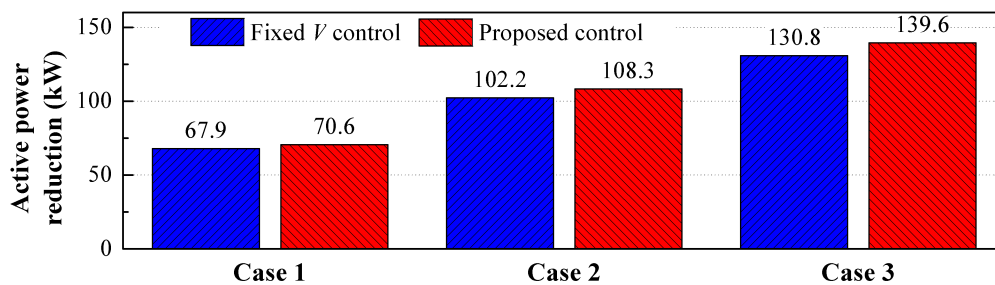


Figure 14. Average reduction of the active power drawn from substation: five-DG system.

6. Conclusions

A CVR method for a distribution system with intermittent DGs is proposed for a next-generation DMS. The requirements for the local reactive power controller of the DG to improve the CVR effect are derived. Based on the requirements, a two-segment Q - P droop controller complying with IEEE Std. 1547TM is proposed. Considering the intermittency, a method to determine the power references for the proposed controller from the optimal solution of the OPF representing CVR is presented. A droop constants determination method is also proposed to maximize the CVR effect while preventing the under-voltage violations. With the proposed method, the power references and droop constants for the proposed reactive power controller are determined periodically by solving the OPF in the DMS and the reactive power output of the DG is adjusted by the proposed local controller in real-time. In the case study, it is verified that the voltages of the test system are maintained as greater than or equal to the lower voltage bound, even though the active power outputs of the DGs are varied. Furthermore, compared with the conventional reactive power control methods, the CVR effect is improved by optimizing the CVR effect at the expected operating point.

Acknowledgments: This work was supported by Korea Electric Power Corporation and Chonnam National University (Project title: Demonstration of energy new business through the smart energy campus).

Author Contributions: Pyeong-Ik Hwang proposed the main idea and wrote the paper. Seung-II Moon checked the overall logic of this work. Seon-Ju Ahn supervised this work and revised the paper.

Conflicts of Interest: The authors declare no conflict of interest.

References

1. Meliopoulos, A.P.S.; Polymeneas, E.; Tan, Z.; Huang, R.; Zhao, D. Advanced distribution management system. *IEEE Trans. Smart Grid* **2013**, *4*, 2109–2117. [CrossRef]
2. Song, I.-K.; Yun, S.-Y.; Kwon, S.-C.; Kwak, N.-H. Design of smart distribution management system for obtaining real-time security analysis and predictive operation in Korea. *IEEE Trans. Smart Grid* **2013**, *4*, 375–382. [CrossRef]
3. American National Standard for Electric Power Systems and Equipment—Voltage Ratings (60 Hz). Available online: <https://www.nema.org/Standards/ComplimentaryDocuments/Contents-and-Scope-ANSI-C84-1-2011.pdf> (accessed on 1 May 2016).
4. Preferred Voltage Levels for AC Systems, 0 to 50 000 V. Available online: <https://www.scc.ca/en/standards/work-programs/csa/preferred-voltage-levels-for-ac-systems-0-50-000-v> (accessed on 1 May 2016).
5. Wang, Z.; Wang, J. Review on implementation and assessment of conservation voltage reduction. *IEEE Trans. Power Syst.* **2014**, *29*, 1306–1315. [CrossRef]
6. Preiss, R.F.; Warnock, V.J. Impact of voltage reduction on energy and demand. *IEEE Trans. Power App. Syst.* **1978**, *5*, 1665–1671. [CrossRef]
7. Sunderman, W.G. Conservation voltage reduction system modeling, measurement, and verification. In Proceedings of Transmission and Distribution Conference and Exposition (T&D), Orlando, FL, USA, 7–10 May 2012; pp. 1–4.
8. Short, T.A.; Mee, R.W. Voltage reduction field trials on distributions circuits. In Proceedings of Transmission and Distribution Conference and Exposition (T&D), Orlando, FL, USA, 7–10 May 2012.

9. Nam, S.R.; Kang, S.H.; Lee, J.H.; Ahn, S.J.; Choi, J.H. Evaluation of the effects of nationwide conservation voltage reduction on peak-load shaving using SOMAS data. *Energies* **2013**, *6*, 6322–6334. [[CrossRef](#)]
10. Vega-Fuentes, E.; Cerezo-Sánchez, J.M.; Rosario, S.L.; Vega-Martínez, A. Voltage reduction field test on a distribution substation. *Int. J. Electr. Energy* **2015**, *3*, 1–5. [[CrossRef](#)]
11. Farivar, M.; Clarke, C.R.; Low, S.H.; Chandu, K.M. Inverter VAR control for distribution systems with renewables. In Proceedings of IEEE International Conference on Smart Grid Communications, Brussels, Belgium, 17–20 October 2011; pp. 457–462.
12. Farivar, M.; Neal, R.; Clarke, C.; Low, S.H. Optimal inverter VAR control in distribution systems with high PV penetration. In Proceedings of IEEE Power and Energy Society General Meeting, San Diego, CA, USA, 22–26 July 2012; pp. 1–7.
13. Manbachi, M.; Nasri, M.; Shahabi, B.; Farhangi, H.; Palizban, A.; Arzanpour, S. Real-time adaptive VVO/CVR topology using multi-agent system and IEC 61850-based communication protocol. *IEEE Trans. Sustain. Energy* **2014**, *5*, 587–596. [[CrossRef](#)]
14. Go, S.I.; Ahn, S.J.; Choi, J.H.; Jung, W.W.; Chu, C.M. Development and test of conservation voltage reduction application for Korean smart distribution management system. In Proceedings of IEEE Power & Energy Society General Meeting, Denver, CO, USA, 26–30 July 2015; pp. 1–5.
15. Manbachi, M.; Farhangi, H.; Arzanpour, S. Smart grid adaptive energy conservation and optimization engine utilizing particle swarm optimization and fuzzification. *Appl. Energy* **2016**, *174*, 69–79. [[CrossRef](#)]
16. Soroudi, A.; Siano, P.; Keane, A. Optimal DR and ESS scheduling for distribution losses payments minimization under electricity price uncertainty. *IEEE Trans. Smart Grid* **2016**, *7*, 261–272. [[CrossRef](#)]
17. Soroudi, A.; Amraee, T. Decision making under uncertainty in energy systems: State of the Art. *Renew. Sustain. Energy Rev.* **2013**, *28*, 376–384. [[CrossRef](#)]
18. Panosyan, A.; Walling, R.; Barthlein, E.-M.; Witzmann, R. Reactive power compensation of self-induced voltage variations. In Proceedings of Integration of Renewables into the Distribution Grid, CIRED 2012 Workshop, Lisbon, Portugal, 29–30 May 2012; pp. 1–4.
19. Smith, J.W.; Sunderman, W.; Dugan, R.; Seal, B. Smart inverter volt/var control functions for high penetration of PV on distribution systems. In Proceedings of IEEE Power Systems Conference and Exposition, Phoenix, AZ, USA, 20–23 March 2011; pp. 1–6.
20. IEEE Standard for Interconnecting Distributed Resources with Electric Power Systems. Available online: http://ieeexplore.ieee.org/xpl/articleDetails.jsp?arnumber=1225051&filter=AND%28p_Publication_Number:8676%29 (accessed on 1 May 2016).
21. Ahmadi, H.; Marti, J.R.; Dommel, H.W. A framework for volt-VAR optimization in distribution systems. *IEEE Trans. Smart Grid* **2015**, *6*, 1473–1483. [[CrossRef](#)]
22. Wood, A.J.; Wollenberg, B.F. *Power Generation, Operation, and Control*; John Wiley & Sons, Inc.: New York, NY, USA, 1996.
23. Bracale, A.; Caramia, P.; Carpinelli, G.; Di Fazio, A.R.; Ferruzzi, G. A Bayesian method for short-term probabilistic forecasting of photovoltaic generation in smart grid operation and control. *Energies* **2013**, *6*, 733–747. [[CrossRef](#)]
24. Advanced Inverters for Distributed PV: Latent Opportunities for Localized Reactive Power Compensation. Available online: http://www.clean-coalition.org/site/wp-content/uploads/2013/10/CC_PV_AI_Paper_Final_Draft_v2.5_05_13_2013_AK.pdf (accessed on 1 May 2016).
25. Kundur, P. *Power System Stability and Control*; McGraw-Hill: New York, NY, USA, 1994.
26. Distribution Test Feeders. Available online: <http://ewh.ieee.org/soc/pes/dsacom/testfeeders/index.html> (accessed on 1 May 2016).
27. Torres, G.L.; Quintana, V.H. An interior point method for nonlinear optimal power flow using voltage rectangular coordinates. *IEEE Trans. Power Syst.* **1998**, *13*, 1211–1218. [[CrossRef](#)]
28. Venkataraman, P. *Applied Optimization with MATLAB Programming*; John Wiley & Sons, Inc.: New York, NY, USA, 2009.
29. Cheng, C.S.; Shirmohammadi, D. A three-phase power flow method for real-time distribution system analysis. *IEEE Trans. Power Syst.* **1995**, *10*, 671–679. [[CrossRef](#)]
30. Hwang, P.I.; Moon, S.I.; Ahn, S.J. A vector-controlled distributed generator model for a power flow based on a three-phase current injection method. *Energies* **2013**, *6*, 4269–4287. [[CrossRef](#)]

31. Moghaddas-Tafreshi, S.M.; Mashhour, E. Distributed generation modeling for power flow studies and a three-phase unbalanced power flow solution for radial distribution systems considering distributed generation. *Electr. Power Syst. Res.* **2009**, *79*, 680–686. [[CrossRef](#)]
32. Ettoumi, F.Y.; Mefti, A.; Adane, A.; Bouroubi, M.Y. Statistical analysis of solar measurements in Algeria using beta distributions. *Renew. Energy* **2002**, *124*, 28–33.



© 2016 by the authors; licensee MDPI, Basel, Switzerland. This article is an open access article distributed under the terms and conditions of the Creative Commons Attribution (CC-BY) license (<http://creativecommons.org/licenses/by/4.0/>).